Target Parameter Estimation using Compressive Measurements

Ameya Anjarlekar 170070013
Sai Gaurav Anugole 170070008
Ram Prakash Sri Sai Seeram 170070047

Instructor : Professor Vikram Gadre
Guide : Nikhar Rakhashia, Shrikant Sharma

April 2020

1 Problem Statement

The number of targets simultaneously present in the visible region of the radar (n_{T}) is much less than the number of pulses (N_{pulse}). Hence, the received signal, which consists of Doppler and micro Doppler frequencies due to rigid body motion and micro motions respectively, can be considered sparse. The received signal in baseband after down-conversion is given by (1).

$$x(t) = \sum_k A_k \exp(j(2\pi t f_{d_k} + \cos(2\pi t f_{m_k}))) + w(t) \tag{1}$$

where A_k's are the signal amplitudes, f_{d_k}'s are the corresponding Doppler frequencies, f_{m_k}'s are the corresponding micro Doppler frequencies and $w(t)$ is White Gaussian Noise.

To exploit the sparsity, we intend to transmit only m out of total N pulses ($N_{\mathrm{T}} < m < N$) to reduce the computational load.

Mathematically, the problem can be described as a graded problem with different grades:

1. Estimate B in $x(t) = \exp(j\{\omega t + B\cos(\omega_1 t)\})$, when ω and ω_1 are known.
2. Estimate B, ω and ω_1 in $x(t) = \exp(j\{\omega t + B\cos(\omega_1 t)\})$.
3. Estimate B, ω and ω_1 in presence of noise. $x(t) = \exp(j\{\omega t + B\cos(\omega_1 t)\}) + w(t)$.
4. Estimate B_i, ω_i and ω_{1_i} in $x(t) = \sum_{i=1}^{N} \left(\exp(j\{\omega_i t + B_i \cos(\omega_{1_i} t)\})\right) + w(t)$.

5. Estimate B, ω and ω_1 in $x(t) = \cos(\{\omega t + B\cos(\omega_1 t)\})$.

Currently, we are estimating ω and ω_1 with all parameters, B, ω and ω_1 unknown for a superposition of complex exponentials in presence of noise i.e. statement number 4 given above.
The work has also been replicated for real sinusoids with satisfactory results. We are modifying the algorithm to improve results further for real sinusoids.

2 Signal Reconstruction using Compressed Sensing (CS) and Fourier basis representation

2.1 Fourier Analysis of FM Signals

For an FM signal represented by

$$s(t) = A\cos(2\pi f_c t + \beta\sin(2\pi f_m t)) \tag{2}$$

Its Fourier Transform $S(f)$ is represented by

$$S(f) = \frac{A}{2}\sum_{n=-\infty}^{\infty} J_n(\beta)[\delta(f - f_c - nf_m) + \delta(f + f_c + nf_m)] \tag{3}$$

where J_n is the Bessel function of order n.

2.2 CS Preliminaries

We consider an undersampled version of $x(t)$ with 20% of total samples required to satisfy Nyquist criteria. Consider X to be a vector consisting of all the total samples of $x(t)$ while Y to be a vector consisting of observed samples of $x(t)$. Then Y can be represented by

$$Y = \Phi X \tag{4}$$

Consider Y to be a $m \times 1$ matrix while X to be a $n \times 1$ matrix. Further we write X in terms of its Fourier coefficients. Thus $X = F\Theta$ where F is the Fourier Basis Matrix $(n \times n)$ and Θ represents Fourier coefficients of x. Thus, we obtain

$$Y = A\Theta \tag{5}$$

where $A = \Phi\Theta$. If Θ is sufficiently sparse and A is sufficiently incoherent, then a sufficiently accurate estimate of Θ can be obtained. This is obtained using Basis Pursuit Algorithms such as OMP, ISTA, CoSAMP etc. In our implementation we are using OMP algorithm.
Once Θ is obtained, X can be obtained through $X = F\Theta$.

2.3 Parameter Estimation

2.3.1 Conjugate multiplication

Let $\hat{x}(t)$ be the signal reconstructed using OMP algorithm from reduced number of received samples. We multiply $\hat{x}(t)$ by the conjugate of its time shifted version.

$$C(t) = \hat{x}(t)\hat{x}^*(t-\tau) \tag{6}$$
$$= \sum_k A_k^2 \exp[j(2\pi\tau f_{d_k})] \cdot \exp\left[4\pi j \cdot \sin\left(\frac{\tau f_{m_k}}{2}\right)\cos\left(2\pi t f_{m_k} - \frac{\tau f_{m_k}}{2}\right)\right] + R(t)$$

where $R(t)$ represents the cross terms. We consider difference in values of f_d to be greater than the maximum value of f_m. Thus, writing $c(t)$ in its Fourier Transform domain using Eq. 3, we get that the peaks in the Fourier Transform of R(t) will be much farther than the peaks due to $\exp(j\sin(.))$ terms. Thus, we can focus only on the peaks due to $\exp(j\sin(.))$ terms. Using the algorithm mentioned below, we can obtain corresponding micro-Doppler frequencies.

2.3.2 Algorithm

1) τ is adjusted such that the peaks at $\pm f_{m_k}$ are significant i.e. the corresponding $J_1(\beta)$ associated with all the micro-doppler frequencies are significant.
For example, suppose the micro-doppler frequencies were 5 and 12 Hz. We adjust τ such that $J_1(\beta)$ is high and thus peaks at -12, -5, 5 and 12 Hz are significant.
2) We consider top k% indices of the total indices in the Fourier Transform array of $C(t)$. Each index represents a particular frequency. Generally we take around 20% of the values. Consider the set of indices to belong to a set S. Further, we sort the indices according to their respective values. We start with the indices with the highest values.
3) We iterate over all the indices in the decreasing order of their values. Consider the current index be f. We check if the top k indices also contain -f. If no, we move to the next index. For example, if a frequency of 6 Hz belongs to S, then we check if -6 also belongs to S. If not, we remove it from set S, else we continue to the next step.
4) If yes, we check if either of 2f and 3f are presented. (We could have also checked the presence of -2f and -3f but we observe empirically that using the above condition is sufficient to accurately estimate the micro-doppler frequencies. Moreover, we are checking either of 2f and 3f since either of $J_2(\beta)$ or $J_3(\beta)$ might be too low for the peak to highlighted in the top k% of the values). For example, since the signal is of the form exp(j sin(.)), if the micro-doppler frequency is 5 Hz, we would have peaks at integer multiples of 5 Hz. Thus, we intend to identify such peaks.
5)If the following indices are present, this implies that f is one of the micro-Doppler frequency. We continue further to find other micro-Doppler frequencies.

2.4 Results

We run a Monte-Carlo simulation for 1000 iterations and check if error between actual f_m and estimated f_m is ≤ 3 for all the targets. We define accuracy along this notion. Following results are obtained for SNR = 10 dB.

Table 1: Accuracy vs Targets

Number of Targets	Accuracy
1	0.958
2	0.993
3	0.882

We also observe that the accuracy increases with the number of measurements. Similar Monte Carlo simulation is run for 1000 iterations to compare the accuracy with the percentage of samples observed. This is performed for number of targets = 1.

Table 2: Accuracy vs Percentage Measurements

Number of Targets	Accuracy
10	0.955
20	0.956
40	0.962

We also observe that the accuracy increases with SNR. Monte Carlo simulation is run for 1000 iterations to compare the accuracy with the SNR of the signal. This is performed for number of targets = 2. We obtain the relationship as shown below.

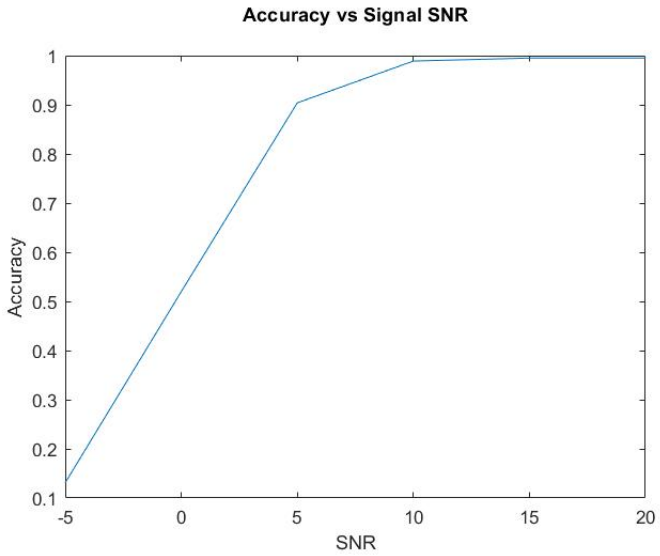

Figure 1: Accuracy vs SNR

3 Estimation of micro-doppler features in single target using wavelet analysis

3.1 Signal Recovery Analysis

The baseband signal received after radar reflection back from a single target and demodulation thereafter, is said to consist of a body-doppler component, from the Doppler frequency shift of the main target body and a micro-doppler component, associated to the sub-motions like rotation of blades or vibrating parts present on the body, which can be mathematically formulated as:

$$s(t) = cos(2\pi f_d t) + cos(2\pi f_d t + \beta cos(2\pi f_m t))$$

where β is the modulation index, f_d and f_m are the body and the micro-doppler frequencies respectively.
The spectrogram plot of such a signal received is of the form as shown below:

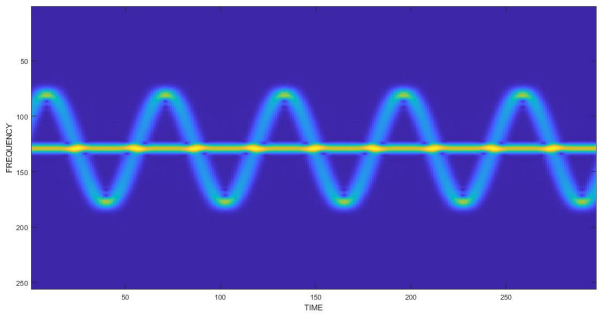

Figure 2: Spectrogram of above signal

The body-doppler component is the constant frequency shift, which can be calculated by simple signal processing techniques while the sinusoidal nature frequency modulated component as seen above represents the micro-doppler part whose characteristics are of interest to us.
Standard spectral analysis techniques like Fourier Transform can't provide time-varying frequency modulation information. Due to unavailability of localized time information, such techniques are not feasible for feature extraction. Therefore, Joint time-frequency techniques are used commonly for these cases. Simple transforms like STFT or other window transforms can be employed however at the cost of lack of resolution for extracting and processing these unique features or cross-term interference. High resolution techniques are necessary and wavelet analysis seems to be a viable approach especially for low signal to noise ratio.
Hence, during the initial stage, a signal of above nature is simulated to extract the m-D frequency, f_m set completely random varying between 1 - 10 Hz, with other quantities fixed. An Additive White Gaussian noise (5 dB) is further added before analysing the signal.
Discrete wavelet transform of the original signal is computed, passing through a multi stage banks (here, 4) of low and high pass digital filters.

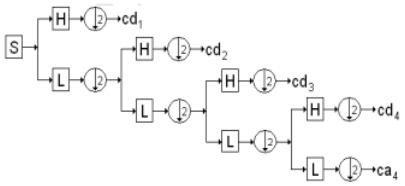

Figure 3: Discrete Wavelet Transform

In this case, the signal $s(t)$ is decomposed using a Daub-4 wavelet for 4 levels finally consisting of a set of approximation coefficients and 4 sets of detail coefficients.

$$s(t) \rightarrow [ca_4, cd_1, cd_2, cd_3, cd_4]$$

Required information from such components are extracted by reconstructing the signal back with only fewer levels of coefficients. In this case, the high frequency components of the original signal is now present in the higher detail levels. Hence, Information regarding the micro-doppler frequency is extracted from the signal reconstructed using higher level coefficients by Inverse Wavelet Transform.

$$[cd_3, cd_4] \rightarrow [D_3, D_4] = r(t)$$

The resulting signal r(t) is auto-correlated to extract the frequency from the periodic peaks observed. For better analysis, peaks are calculated from the envelope of the auto-correlation function.

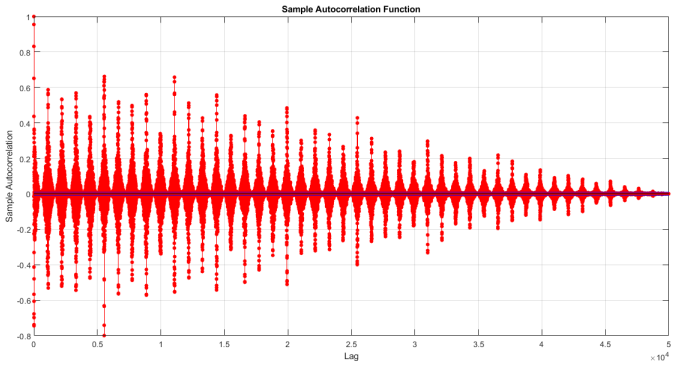

Figure 4: Auto-correlation of r(t)

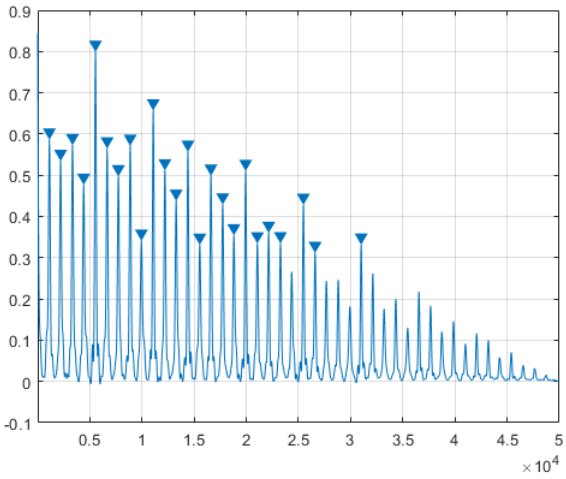

Figure 5: Envelope and peaks of r(t)

The frequency f_m is calculated from the distance between the adjacent peaks. Accuracy of estimation of f_m is calculated by selecting a random value of f_m and detecting it after the analysis. For over 100 iterations, this approach was able to estimate the frequency within an error limit of 0.5 Hz from the actual value, around 90 times on average.

3.2 Feature Extraction using models in MATLAB

In this stage, a moving helicopter (target) is simulated using models present in MATLAB. Features like blade rate, length, number of blades are added to determine these quantities from the micro-doppler signatures of radar return signal. The trans receiver point, modulation of signal, etc has been done to relate to a real-life working mechanism.

3.2.1 Parameters of the model

- **Radar Position and velocity :** The location of radar unit that transmits/receives the signal and its velocity components if any are mentioned in 3-d coordinates. Zero velocity is given for a stationary source
- **Target Position and velocity :** The initial position of the target and its velocity is given. The target motion is induced via a Platform system object for translation
- **Micro Doppler Features :** This includes the number of blades, their lengths and rotation rates are mentioned. Target cross-section areas are then given to the main body and the blades in the ratio of 10:1 which shall

later be responsible for the amplitude of reflected radar signal received before processing. This is implemented using Radar Target system object which models the response of the signal returned. The propagating speed in the medium ($c = 3 \times 10^8 m/s$) and signal carrier frequency, 5GHz is used.

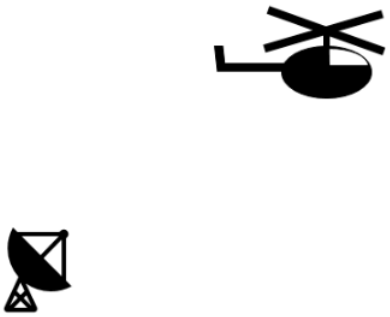

Figure 6: Radar and the moving target

- **Transmitting Waveform :** The nature of transmitted signal is chosen to be of pulsed type wherein series of pulses are transmitted for limited duration. For simulation purposes, a single rectangular pulse, with $2\mu s$ pulse-width, with signal sampling frequency, $f_s = 1MHz$ is chosen using Rectangular Waveform system object.

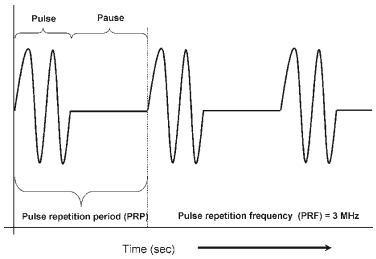

Figure 7: Pulse repetition waveform

- **Echo Simulation :** Sensor arrays or a group of sensors in a geometric pattern are usually employed in the radar for collecting and processing of electromagnetic signals for better estimation purposes. A simple 4×4 uniform rectangular array is implemented using URA object. Signal is transmitted (using Radiator object), modelling a narrowband signal propagation from one point to another in a free-space environment (via FreeSpace object). Reflected signal is received via the Collector object
- **Storage of received information :**The received information after de-

modulation is stored in the form of a matrix with dimensions of number of samples per pulse ($\frac{f_s}{prf} = 50$) and pulsed-times (1000). A Range-Doppler response is also plotted which maps the response of the signal to particular doppler shifts after passing through matched filter based on transmitted waveform. The spread around the main doppler shift indicates the response of the m-D signatures

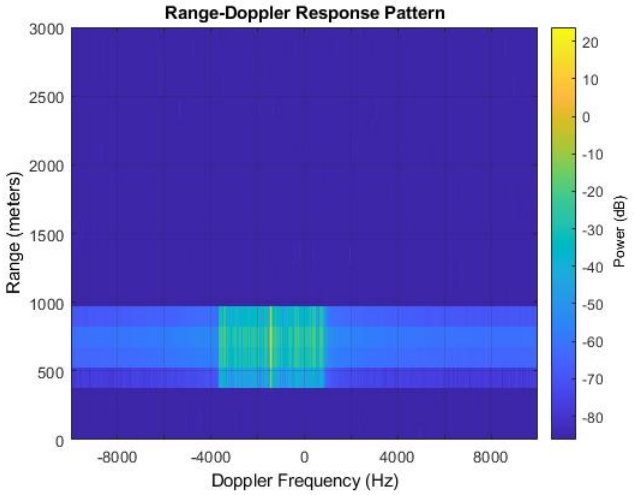

Figure 8: Range Doppler Response

3.2.2 Blade return Analysis

The power spectrum of the received signal corresponding to that pulse with maximum amplitude is further considered for analysis is plotted as shown below:

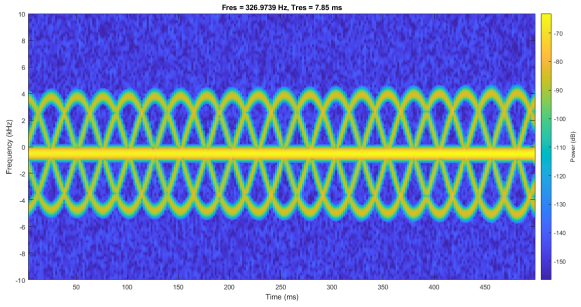

Figure 9: Power Spectrum

The nature of response is expected and is close to a sinusoid frequency modulated signal. Each blade tip introduces a sinusoid-like doppler modulation

3.2.3 Number of blades estimation

The number of peaks within a period of sinusoid is the same as number of blades. Hence, number of peaks over a random time instant is calculated, one less than it (after subtracting the body doppler component) yields the number of peaks. To avoid ambiguities at time-instants where multiple curves meets, the peaks are found for multiple random instants and the maximum is selected.

3.2.4 Maximum Doppler shift

The FFT of the original signal is found, with its spectrum as shown below:

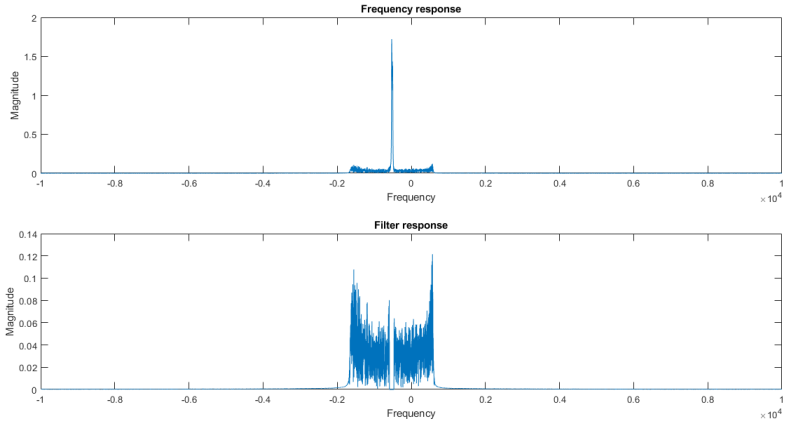

Figure 10: Frequency Responses

Notch filter is applied to remove the main doppler shift. The maximum shift is then calculated from the Filtered response, which shall be later useful for calculation of the blade length. It can be seen that no useful feature can be inferred from the FFT of the signal regarding the m-D signatures.

3.2.5 Blade rate estimation

Wavelet based analysis as done before is employed here to estimate the m-D frequency. The Discrete Wavelet Transform of the signal is found and detail level components are used to reconstruct the response signal using Inverse Transform.

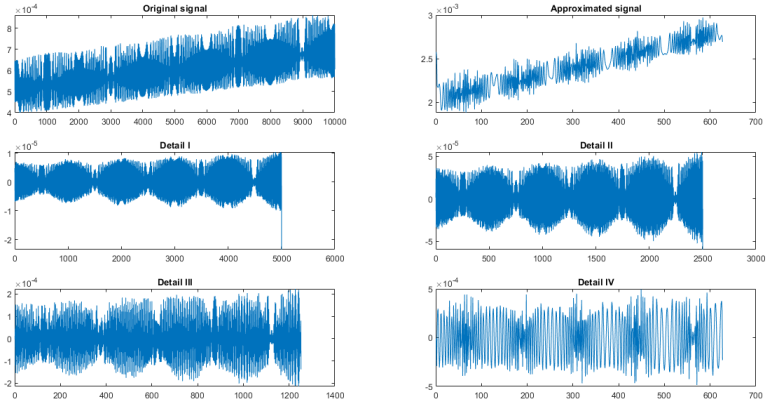

Figure 11: Signal Decomposition using DWT

Auto-correlation is then performed to determine the frequency from the period of the peaks. A simple peak detection algorithm is used to locate the peaks and the distances between them. The Blade rate is then calculated by dividing this with the number of blades.

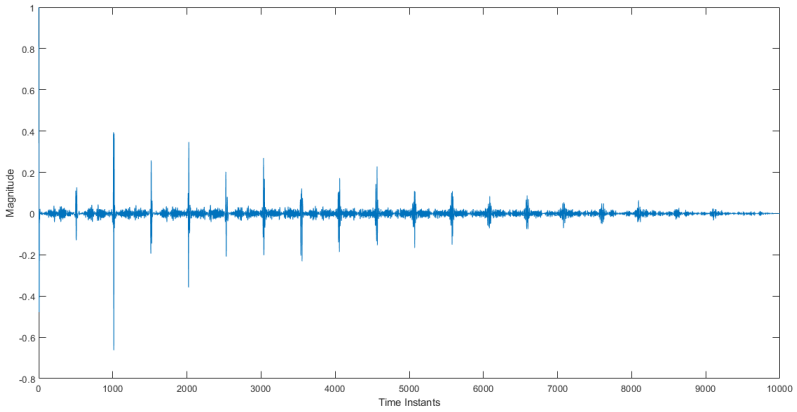

Figure 12: Sample Autocorrelation response

3.2.6 Blade length estimation

The maximum blade tip velocity is determined from the maximum doppler shift which is converted to velocity. This velocity is the component of the actual velocity along the line of reception of the radar signal. Since, the angle of reception is already known to radar, the actual velocity is found by dividing the radial

component with the cosine of the angle.

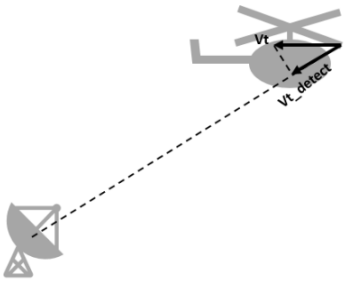

Figure 13: Maximum Tip velocity and its radial component

The blade length is then estimated by dividing the tip velocity with the angular blade velocity found using the blade rate calculated before.

	Actual	Algorithm Output
Number of blades	4	4
Blade rate(in rps)	8.17	7.96
Length of blade (in m)	5.22	5.5

Table 3: Comparision of actual vs algorithm output results

4 Estimation of Rotor Blade Length using Compressive Sensing

4.1 Resimulation of the paper[2]

The paper tries to estimate the rotor rps and blade length of a drone with 2 blades on a fixed platform. Because of the rotating blades, when we transmit a wave, we expect to that the reflected will have a micro doppler component. But unlike the case of point-like particle, in the experiment conducted, because of the fairly close distance between the radar and the target(about 1.5m) point-like particle cannot be assumed and we must integrate the reflections from different parts of the blade to get an analytical expression for the reflected wave. The resulting reflected wave has the expression[2]

$$s_{reflected}(t) = Lexp\left[-j\frac{4\pi}{\lambda}[R_0 + z_0 sin\beta]\sum_{k=0}^{N_b-1} exp(-j\psi_k(t))sinc(\psi_k(t))\right]$$

where

$$\psi_k(t) = \frac{4\pi L}{2\lambda} cos\beta cos(\Omega t + \phi_0 + 2\pi k/N_b)$$

and L = Length of the blade, λ = wavelength of transmitted wave, R_0 = Target distance on ground, z_0 = Target alevation, β = Alevation angle, N_b = Number of blades, Ω = rotor blade angular speed

The paper finds the maximum velocity of a point on the blade and the angular velocity of the blade and then uses them to measure the blade length

4.1.1 Measuring Maximum velocity of all points on the blade

The frequency response of the reflected spectrum extends only up to the maximum doppler shift caused by all points on the blade, which corresponds to the maximum velocity of all points. That is, we can determine the maximum velocity just by finding the bandwidth of the reflected signal Figure 14a,14b. To automatically detect this, the point where the derivative of the envelope of the frequency response is maximum is found. The need for using the envelope was to minimize the affects of noise on the parameter extraction. The maximum velocity is back-calculated from this point as,

$$v_{max} = \frac{\lambda f_{max}}{4\pi cos(\beta)}$$

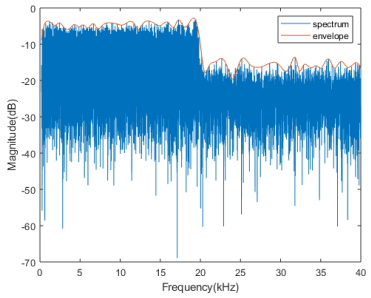

(a) Frequency Response of Reflected Signal

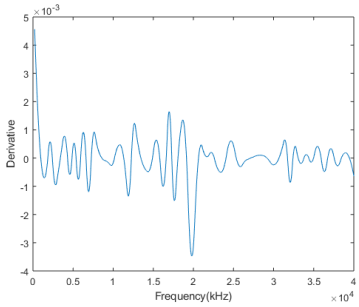

(b) Derivative of envelope of Frequency Response

Figure 14

4.1.2 Measuring fundamental Micro-Doppler Frequency

The paper exploits the fact that the reflected signal has a periodic waveform after applying STFT Figure 15a. To convert the 2D STFT output to a single dimension, the paper finds median power frequency for every instant of time

Figure 15b. Now the median frequency plotted as a function of time yields a periodic function of same frequency as the fundamental micro-doppler frequency

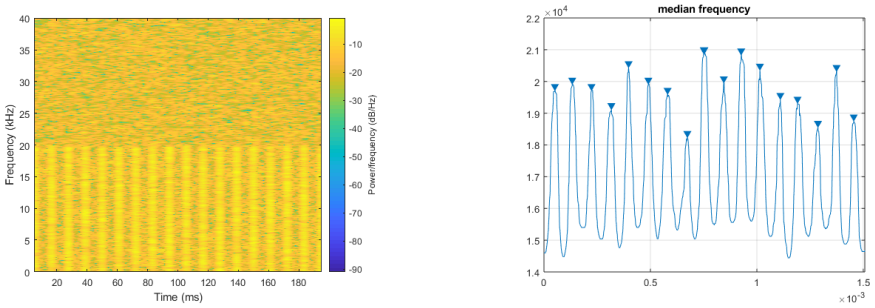

(a) STFT of Reflected wave

(b) Median Frequency of STFT

Figure 15

The fundamental micro-doppler Frequency is given as

$$f_{md} = \frac{1}{N_b * \text{Period of Median Frequency}} = \text{RPS of rotor blade}$$

Finally dividing v_{max} and RPS of rotor blade yields the length of rotor blade

	Actual	Algorithm Output
RPS rotor	45Hz	42.74Hz
Length of blade	11.5cm	11.29cm

Table 4: Comparision of actual vs algorithm output results

Although the method shows great accuracy in measuring the blade length, the simulation of the paper requires 250,000 samples to exatract the parameters sampled at high frequency.

Also incase of multiple targets , we can find v_{max} and RPS of rotor of all the different targets present, it is not possible to correlate which v_{max} corresponds to which RPS and hence cannot compute the rotor blade length

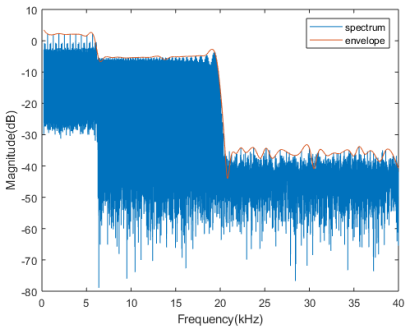

Figure 16: Fourier Transform of reflected wave with two targets

4.2 Compressive Sensing

We turn to compressive sensing to adress the issue of large number of samples required to estimate the parameters.

Unlike the point-like particle case, even with the presence of a sinc, because the sinc itself is also a periodic function in microdoppler frequency, the sparsity of signal is preserved at the cost of doubling of number of non-zero elements in the fourier basis. So compressive sensing with the orthogonal basis as the fourier domain is possible.

We introduce a compressive sensing step to the above approach proposed by the paper. Rather than, finding all the samples, we only use m samples where sparsity of signal ¡ m ¡ total samples and them apply compressive sensing algorithms(OMP in this case) to reconstruct the signal. Then we can apply the algorithm proposed by the paper to find the rotor blade length

The following results(Table 5, Figure 17) are at SNR = 10 and 20% compression(that is only 20% of the samples are used to extract blade length). The wavelength of the transmitted wave is decreased to increase the sparsity of the reflected signal and increase processing time of OMP

	Actual	Algorithm Output
RPS rotor	45Hz	42.8Hz
Length of blade	11.5cm	10.7cm

Table 5: Comparision of actual vs algorithm output results

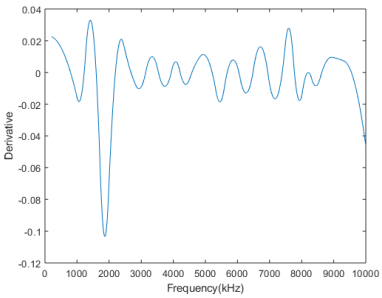

(a) Derivative of Envelope of Frequency Response of Reflected wave

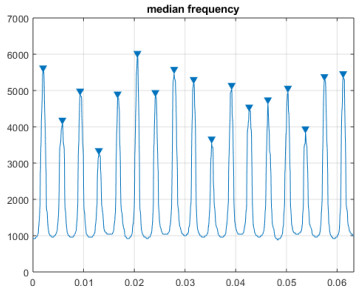

(b) Median Frequency of STFT of reflected wave

Figure 17: Compressive Sensing

The Compressive Sensing step introduced reduces the number of samples required to be read at the cost of post-processing time. The OMP algorithm takes time proportional to the number of samples for execution.

Also the compressive sensing step does not handle the multi-target case just like the paper's approach. Moving forward, a new approach can be found to handle the multi-target case so that the algorithm can be implemented in a practical scenario

References

[1] Micro-Doppler Effect in Radar: Phenomenon, Model, and Simulation Study - *V.C.Chen, Fayin Li, Shen-Shyang Ho and Harry Wechsler*

[2] Automatic Measurement of Blade Length and Rotation Rate of Drone Using W-Band Micro-Doppler Radar - *Ashish Kumar Singh and Yong-Hoon Kim*

[3] Compressed Sensing - *David L. Donoho*

[4] Analysis of Radar Micro-Doppler Signatures From Experimental Helicopter and Human Data - *Thayananthan Thayaparan, Sumeet Abrol, Edwin Riseborough, LJubiša Stankovic, Denis Lamothe and Grant Duff*

[5] Radar Target Classification by Micro-Doppler Contributions - *Pavlo Molchanov*